Electronic Supplementary Information for

Flexible and ultra-broadband terahertz wave absorber based on graphene-vertically aligned carbon nanotube hybrids

Dongyang Xiao[a,+], Minmin Zhu[b,c,+], Qian Wang[a], Leimeng Sun[a,*], Chun Zhao[a], Zhi Kai Ng[b], Edwin Hang Tong Teo[b], Fangjing Hu[a,*], Liangcheng Tu[a]

[a]MOE Key Laboratory of Fundamental Physical Quantities Measurement & Hubei Key Laboratory of Gravitation and Quantum Physics, PGMF and School of Physics, Huazhong University of Science and Technology, Wuhan 430074, Hubei, China
[b]School of Electrical and Electronic Engineering, Nanyang Technological University, 50 Nanyang Avenue, Singapore 639798, Singapore
[c]Temasek Laboratories, Research Techno Plaza, 50 Nanyang Drive, Singapore 637553, Singapore
[+]Contributed equally to this work
*Corresponding author
*Email: sunleimeng@hust.edu.cn (L.S) and fangjing_hu@hust.edu.cn (F.H)

Electronic Supplementary Information S1, Raman spectra of VACNT and graphene

The Raman spectra of VACNT on the Si and flexible PET/Cu/PDMS substrates are shown in Figure S1(a), clearly showing the D (1350 cm^{-1}) and G (1570 cm^{-1}) bands associated with the defect of the graphite sheet,[1,2] and the carbon SP^2 structure that reflects the symmetry and degree of crystallinity, respectively. Furthermore, a lower I_D/I_G ratio was obtained on the flexible substrate, which is attributed to the less amount of amorphous carbon on top after the treatment at 500 ℃ temperature under a weak oxidation environment during the transfer process[3]. Figure S1(b) further illustrates the Raman spectra of graphene on the Si/SiO_2 substrate. The same characteristic peaks associated with the D and G bands were identified, as well as the 2D peak (2690 cm^{-1}) originated from two-phonon elastic scattering.

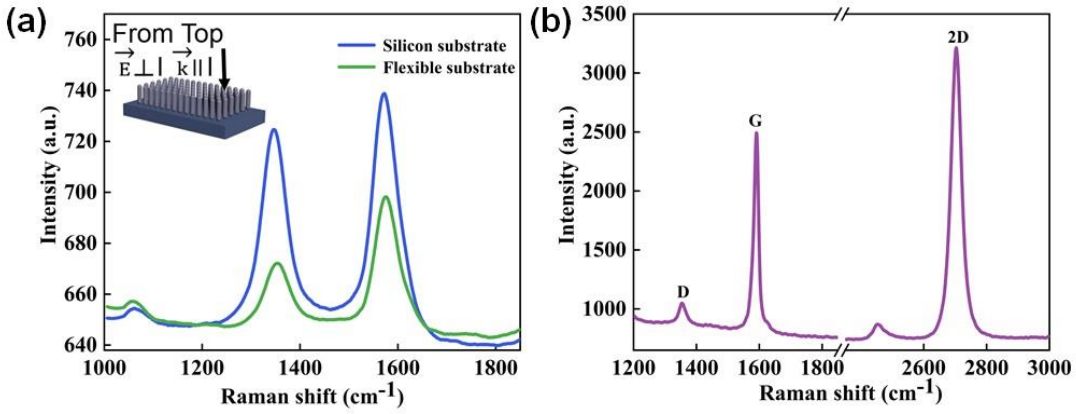

Fig. S1 Raman Spectra of (a) VACNT on Si and flexible PET/Cu/PDMS substrates; (b) graphene on the Si/SiO_2 substrate.

Electronic Supplementary Information S2, CST Simulation setup

The real and imaginary parts of the refractive index of VACNTs were calculated based on Maxwell-Garnett theory according to the optical data of graphite[4]. The results were imported into the commercial electromagnetic simulation software CST to model the VACNT for numerical simulations. PDMS was modelled as a dispersive material with a dielectric constant of 2.35 and loss tangent of 0.05 at 1.0 THz[5]. The optical properties of graphene layer, i.e., tranmisttance and reflectance, were calculated using the embedded Macro "Graphene Material for Optical Applications", and the chemical potential was set to 0.3 eV.

In CST, the time-domain solver was used to obtain the broadband electromagnetic response of the absorber. The boundary conditions in *x*- and *y*- direction were set to the electric and magnetic walls, respectively, to mimic an infinite VACNT array, while open boundary was employed in the *z*-direction. The waveports were placed 1000 μm away from the structure, and the size of meshes were set to 1/10 wavelength with respect to 3 THz to ensure a high simulation accuracy. After obtaining the voltage reflection coefficient at the input port (S_{11}), the power reflectance $R = |S_{11}|^2$ and power absorptance $A = 1 - R$ can be derived as the power transmittance $T = |S_{21}|^2 = 0$ due to the existence of ground Cu layer.

Electronic Supplementary Information S3, Power loss density within stacked layers

In order to identify the contribution of each layer to the overall power absorptance of the proposed THz absorber, power loss densities were simulated using CST for t_{VACNT} = 50, 100 and 200 μm, respectively, as shown in Figure S2. It can be seen that a majority of energy of energy of the incident THz wave is absorbed by the VACNT layer. For t_{VACNT} = 50 μm, the PDMS substrate and graphene layer also play an important role in improving the overall power absorptance. As t_{VACNT} increases to 200 μm, most energy of the incident THz waves can be absorbed by the top VACNT layer, as evidenced by a lower power loss density in the PDMS substrate. This agrees well with simulated and measured power absorptance shown in Figure 5c and Figure 5d.

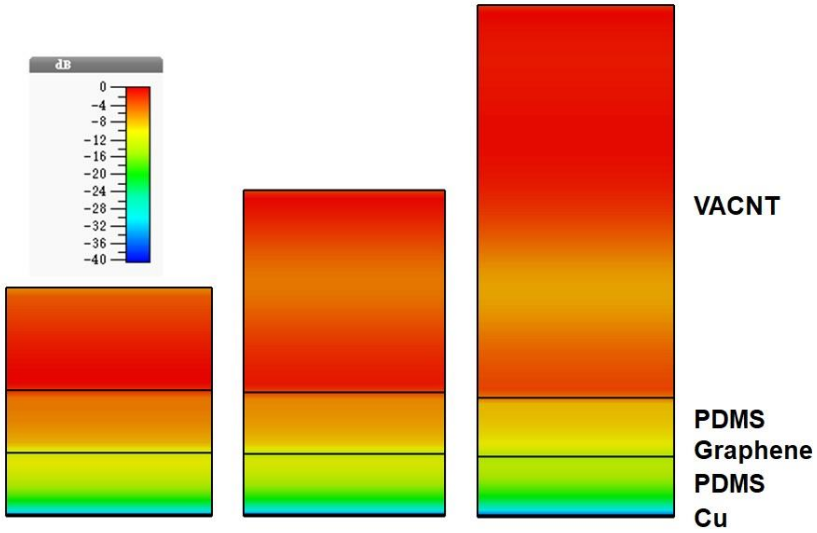

Fig. S2 Simulated power loss density for the proposed THz absorber with t_{VACNT} = 50, 100 and 200 μm, respectively.

Electronic Supplementary Information S4, Schematic illustration of the absorber in bending state

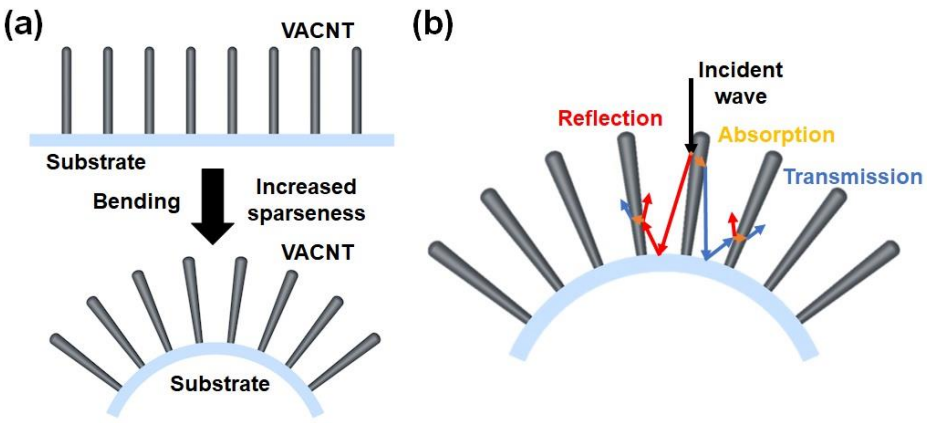

Fig. S3 Schematic illustration of the absorber in bending state and reasons for improved power absorptance. (a) Increased sparseness. (b) Multiple reflections.

References

1. Dresselhaus, M.; Jorio, A.; Saito, R. Characterizing Graphene, Graphite, and Carbon Nanotubes by Raman Spectroscopy. *Annu. Rev. Condens. Matter Phys*. 2010, 1, 89–108.
2. Beams, R.; Cançado, L. G.; Novotny, L. Raman Characterization of Defects and Dopants in Graphene. *Journal of Physics: Condensed Matter* 2015, 27, 083002.
3. Wang, M.; Li, T.; Yao, Y.; Lu, H.; Li, Q.; Chen, M.; Li, Q. Wafer-Scale Transfer of Vertically Aligned Carbon Nanotube Arrays. *Journal of the American Chemical Society* 2014, 136, 18156–18162.
4. Lehman, J.; Yung, C.; Tomlin, N.; Conklin, D.; Stephens, M. Carbon Nanotube-Based Black Coatings. *Appl. Phys. Rev*. 2018, 5, 011103.
5. Luo, X. *Engineering Optics 2.0: A Revolution in Optical Theories, Materials, Devices and Systems*; Springer Verlag, Singapore, 2019.